PS-9-06
Extended Abstracts of the 2018 International Conference on Solid State Devices and Materials, Tokyo, 2018, pp1201-1202

Magnetization Vector Dependence of Berry-Phase Effect in MnAs Films

Hailong Wang*, Jialin Ma, Xiaolei Wang, Dahai Wei and Jianhua Zhao

State Key Laboratory of Superlattices and Microstructures, Institute of Semiconductors, Chinese Academy of Sciences
P. O. Box 912, Beijing 100083, China
Phone: +86-134-0110-4817 E-mail: allen@semi.ac.cn

Abstract

The magnetization vector dependence of Berry-phase effect in epitaxial MnAs films has been systematically investigated. With the magnetization direction rotating from MnAs [01-10] to [0001], the magnetization magnitude dependence of the Berry-phase effect presents a linear to nonlinear crossover. The corresponding physical origins have been clarified, in which the linear behavior is attributed to the spin-flip scattering process, while the nonlinear behavior results from a mixed contribution of spin-flip scattering and Kondo-like skew scattering.

1. Introduction

As one of the frontiers in condensed matter physics, Berry-phase effect has been widely studied due to its abundant physical connotation [1-3]. Based on this notion, a deeper understanding for the intrinsic anomalous Hall effect (AHE) has been established in recent years [3-6]. So far, great efforts have been devoted to clarifying the correlation between Berry-phase contribution and magnetization vector[7-9]. However, a clear physical picture for the dependence of Berry-phase effect on the magnetization magnitude is still in debate.

Epitaxial MnAs films offer the possibility to address the above issues since it has several unique advantages. Firstly. high-quality MnAs films with different orientations can be obtained by changing the orientations of the GaAs substrates, providing us the capability to investigate the magnetization magnitude and direction dependence of the Berry-phase effect in one material. Secondly, the influence of current direction on Berry-phase effect can also be conveniently determined in MnAs films. Thirdly, a crossover between the localized and itinerant electronic behaviors was found in MnAs, which makes it possible to reveal the correlation of the electronic transport properties and the specific form of the magnetization vector dependent Berry-phase effect.

In this work, the magnetization magnitude dependence of Berry-phase effect is found to be greatly affected by the magnetization direction in MnAs films, while the influence of current direction is minor.

2. Experiments and Results

Two sets of MnAs films orienting [01-10] and [0001] with different thicknesses were grown on GaAs (001) and (111)B substrates by molecular-beam epitaxy. For clarity, the 16 nm, 20 nm, 40 nm thick MnAs (01-10) films (set-A) and 16 nm, 20 nm thick MnAs (0001) films (set-B) are named A1, A2, A3, B1 and B2, respectively. Besides, the MnAs [2-1-10], [01-10] and [0001] directions are labelled as MnAs ***a***, ***d*** and ***c*** axes. The epitaxial relationships between MnAs films and GaAs substrates with different orientations are schematically shown in Fig. 1.

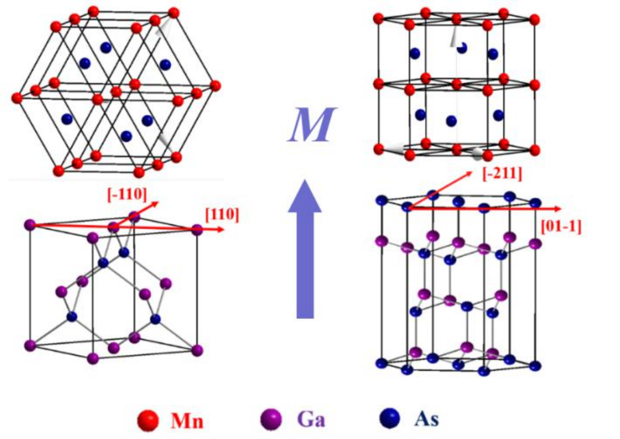

Fig. 1 Crystal structures and epitaxial relationships of MnAs deposited on GaAs with orientations of (a) (001) and (b) (111)B.

Figure 2(a) presents the temperature dependence of normalized remnant magnetization for two typical samples, A1 and B1. The transition temperatures accompanied by a complete first-order structural phase transition are determined to be ~ 320 K and ~ 350 K for set-A and set-B samples, respectively. Additionally, the magnetic hysteresis loops for the above two samples measured along MnAs ***a*** axis at 5 K are shown in Fig. 2(b). Obviously, the magnetic easy axis featuring a square loop is always parallel with MnAs ***a*** axis for these two sets of samples.

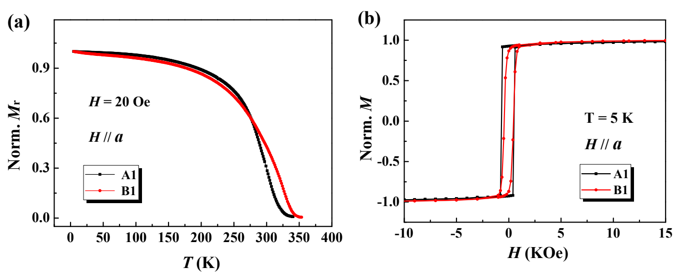

Fig. 2 (a) Temperature dependence of the remnant magnetization. (b) Normalized magnetic hysteresis loops at 5 K for A1 and B1.

Figure 3(a,b) plots the temperature dependence of the longitudinal (Hall) resistivity for samples A1, A2 and A3. The intrinsic anomalous Hall conductivity γ can be extracted as the slope by linearly fitting the ρ_{AH} versus ρ^2 curves. The $(\rho/\rho_{300K})^2$ dependence of ρ_{AH} for three set-A samples are plotted in Fig. 3(c). It is evident that the linear behavior between ρ_{AH} and $(\rho/\rho_{300K})^2$ for each film is only maintained at low temperatures (approximately from 5 K to 175 K). The deviation from the linear behavior is obvious at relatively high temperatures, implying the significant effect of the decreased magnetization magnitude. Generally, γ is a function of $|M|$, i.e. $\gamma \propto |M|^k$, in which k is a dimensionless constant. Figure 3(d) presents the $(\rho_{AH}/|M/M_0|)$ versus $(\rho/\rho_{300K})^2$ curves, in which $|M_0|$ stands for the magnetization magnitude at 5 K. As can be seen, the linear relationship between $(\rho_{AH}/|M/M_0|)$ and $(\rho/\rho_{300K})^2$ spans a broad temperature interval of around 300 K, indicating that γ is proportional to $|M|$. γ is then extracted by linearly fitting the $(\rho_{AH}/|M/M_0|)$ versus $(\rho/\rho_{300\ K})^2$ curve and determined to be about 150 Ω-1·cm-1, which is consistent with that obtained from the low temperature data .

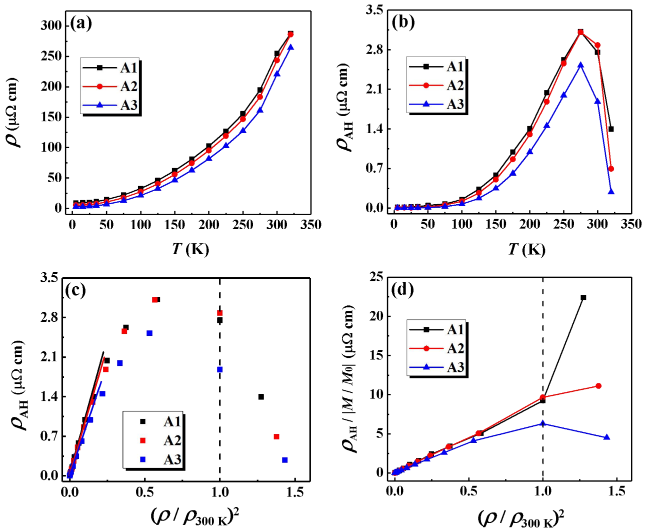

Fig. 3 Temperature dependence of the (a) longitudinal and (b) anomalous Hall resistivity. (c) ρ_{AH} and (d) $(\rho_{AH}/|M/M_0|)$ as a function of $(\rho/\rho_{300K})^2$ for samples A1, A2 and A3

Figure 4(a) shows the $(\rho/\rho_{300\ K})^2$ dependence of ρ_{AH} for samples B1 and B2, respectively. At first, $\gamma \propto |M|$ is considered, and the $(\rho_{AH}/|M/M_0|)$ versus $(\rho/\rho_{300K})^2$ curves for set-B samples are plotted in Fig. 4(b). However, each curve can only be fitted by a linear function in the low-temperature region, which is obviously different with the set-A samples. Therefore, there should be an additional effect induced by the increased temperature in this case. It is found that the $(\rho_{AH}/|M/M_0|^{1.5 \pm 0.1})$ versus $(\rho/\rho_{300\ K})^2$ curves can be well fitted by a linear function from 5 K to 300 K [Fig. 4(c)], which suggests the relationship of $\gamma \propto |M|^{1.5 \pm 0.1}$ (i.e. $k = 1.5 \pm 0.1$) in set-B samples. Compared with the relationship of $\gamma \propto |M|$ in set-A samples, the remarkable influence of the magnetization direction on the magnetization magnitude dependence of Berry-phase effect is confirmed.

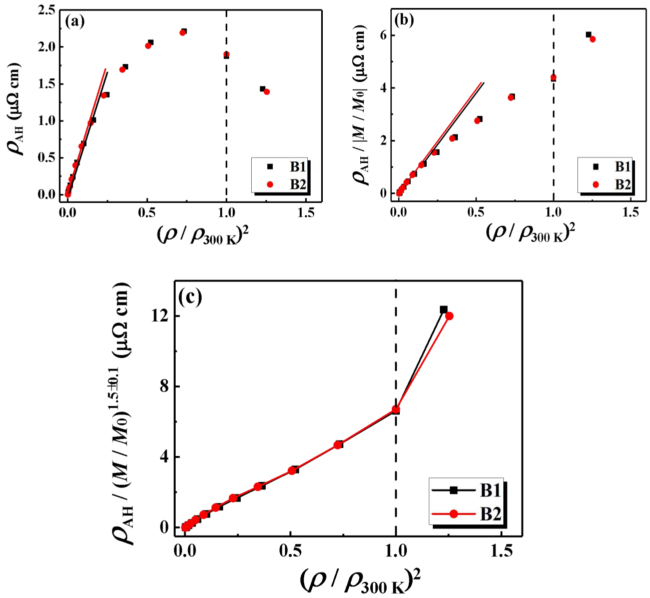

Fig. 4 Dependence of (a) ρ_{AH}, (b) $(\rho_{AH}/|M/M_0|)$ and (c) $(\rho_{AH}/|M/M_0|^{1.5 \pm 0.1})$ on $(\rho/\rho_{300K})^2$ for samples B1 and B2.

3. Conclusions

In conclusion, the magnetization vector dependence of Berry-phase effect in hexagonal MnAs films has been investigated. A linear (nonlinear) function between the Berry-phase effect and magnetization magnitude tuned by temperature has been observed with the magnetization direction along MnAs ***d*** (***c***) axis. The linear behavior is attributed to the spin-flip scattering, while the nonlinear behavior to a mixing mechanism of spin-flip scattering and Kondo-like skew scattering. Our work paves a new avenue for the further investigation of Berry-phase effect and anomalous Hall effect.

Acknowledgements

This work is supported partly by MOST of China (Grant No. 2017YFB0405702) and NSFC (Grants No. U1632264 and 11704374).

References

[1] D. Xiao *et al.*, Phys. Rev. Lett. **97**, 026603 (2006).
[2] Y. Taguchi *et al.*, Science **291**, 2573 (2001).
[3] D. Xiao *et al.*, Rev. Mod. Phys. **82**, 1959 (2010).
[4] N. Nagaosa *et al*, Rev. Mod. Phys. **82**, 1539 (2010).
[5] T. Jungwirth *et al*, Phys. Rev. Lett. **88**, 207208 (2002).
[6] Z. Fang *et al.*, Science **302**, 92 (2003).
[7] C. G. Zeng *et al.*, Phys. Rev. Lett. **96**, 037204 (2006).
[8] Y. G. Yao *et al.*, Phys. Rev. Lett. **92**, 037204 (2004).
[9] R. Mathieu *et al.*, Phys. Rev. Lett. **93**, 016602 (2004).